Regular article

The finding of crystallographic orientation dependence of hydrogen diffusion in austenitic stainless steel by scanning Kelvin probe force microscopy

Zhengli Hua [a,b], Bai An [b,*], Takashi Iijima [b], Chaohua Gu [a], Jinyang Zheng [a]

[a] Institute of Process Equipment, Zhejiang University, Hangzhou, Zhejiang 310027, PR China
[b] National Institute of Advanced Industrial Science and Technology (AIST), Tsukuba, Ibaraki 305-8569, Japan

ARTICLE INFO

ABSTRACT

A combination of scanning Kelvin probe force microscopy (SKPFM) and electron backscatter diffraction (EBSD) has been applied to investigate the hydrogen release from thermally hydrogen-precharged type 304 austenitic stainless steel (γ-SS). The evolution of contact potential difference (CPD) well exhibits the evolution of hydrogen concentration in the near surface area. It is found for the first time that the hydrogen diffusivity in γ-SS depends on the crystallographic orientation. The hydrogen diffusion out from (001) and (101) grains is faster than from (111) grains while no obvious difference is found between (001) and (101) grains.

© 2017 Acta Materialia Inc. Published by Elsevier Ltd. All rights reserved.

Austenitic stainless steels (γ-SS) are promising candidates for structural materials used in high pressure hydrogen service; however, hydrogen embrittlement (HE) has important implications for the applications of γ-SS [1–3]. The HE process is controlled by hydrogen diffusion and accumulation in a local embrittled region, such as ahead of crack tips and grain boundaries [4–6]. Therefore, hydrogen behavior at the micro- and nano-scale is important to fully understand the HE mechanisms. However, the knowledge of hydrogen behavior at micro- and nano-scale, including the crystallographic orientation dependence of hydrogen diffusion in grains, is still lacking because the measurement of localized hydrogen distribution in metal is still a difficult task [7–10]. Recently, scanning Kelvin probe force microscopy (SKPFM), which combines Kelvin probe technology and atomic force microscopy (AFM), has attracted considerable attention because of its capability to detect the variation of contact potential difference (CPD) induced by hydrogen ingress with high spatial resolution [10–14]. The CPD is given by $CPD = (\varphi_{tip} - \varphi_{sample}) / e$, where φ_{tip} and φ_{sample} are the work functions of tip and sample respectively, and e represents the value of the elementary charge [10–14]. Masuda [11] measured the stress corrosion cracking in type 304 γ-SS by SKPFM and attributed the CPD variation to hydrogen produced by cathodic reactions. Larignon et al. [12,13] investigated the hydrogen distribution in cathodically hydrogen-charged aluminum alloy by SKPFM and secondary ion mass spectroscopy (SIMS),

and demonstrated that SKPFM appears to be more flexible than SIMS, with the capability of exploring absorbed hydrogen in aluminum alloys at nano-scale. Senöz et al. [14] measured hydrogen permeation in-situ in a thin Pd foil by SKPFM, and found that the CPD variation depended logarithmically on the amount of hydrogen in the thin Pd foil and was dependent on crystallographic orientation. Unfortunately, they simply attributed the grain orientation dependence of CPD to differences in hydrogen trap density in different grains [14]. Microstructural effects on hydrogen diffusivity in metal has been well known and is attributed to crystal defects, such as vacancies, dislocations, grain boundaries etc., however, the role of crystallography on hydrogen transport remains unclear. In this paper, we investigate the hydrogen distribution and evolution in thermally hydrogen-precharged type 304 γ-SS by a combination of SKPFM and EBSD under controlled conditions, to clarify the dependence of hydrogen diffusion on grain orientation in γ-SS.

Commercially available type 304 γ-SS was used. The material was solution-annealed at 1393 K for 1 h and then machined into plate specimens with a thickness of 1 mm. The specimens were ground with SiC paper up to 2000 grit and ultrasonically cleaned in ethanol, and then charged in 82 MPa gaseous hydrogen at 573 K for 250 h. From Perng and Altstetter's data for hydrogen diffusion [15], hydrogen charging (HC) in 82 MPa H_2 at 573 K for 250 h can result in a uniform equilibrium hydrogen concentration in the specimen.

Before SKPFM measurement, the specimen surface was mechanically polished once again in order to remove the surface segregation layers formed during HC, and finished by Ar-ion milling, which removed the

* Corresponding author.
E-mail address: b.an@aist.go.jp (B. An).

surface layers altered during mechanical polishing. This treatment would cause hydrogen loss from the surface and near surface area, producing a hydrogen content gradient in the surface layer. After Ar-ion milling the specimen was exposed to Lab atmosphere for 10 min and then introduced into a custom made nitrogen vessel which was equipped with a Nanoscope IIIa Multimode scanning probe microscope (SPM). Nitrogen purging in the vessel was performed for more than 1.5 h before testing, in order to minimize the effects of oxygen and humidity which have been known to severely affect CPD [16,17]. Therefore, the SKPFM measurements were generally started after 2 h from the finishing of ion milling. The SKPFM measurements were carried out in the tapping/lift mode with a lift height of 50 nm at 301 ± 0.5 K in the flowing nitrogen atmosphere for three days. Then, the specimens were heated at 473 K for 2.5 h in a vacuum with a pressure of 1.8×10^{-5} Torr to release the precharged hydrogen. The potential calibration of the tip was carried out using an Au sample to avoid the errors caused by the change of the tip character. The discrepancy between CPDs measured at different times (each different approaching of SKPFM probe) for the Au sample was within 0.02 V under our experimental conditions, meaning that the error range of testing at different times is about 0.02 V. The CPD of the hydrogen-charged and annealed specimen and the non-charged specimen were measured by SKPFM after the same processes of specimen preparation. The crystallographic information of the specimens was collected by an Oxford instruments NordlysMax II EBSD system after the SKPFM measurements. The accelerating voltage and step size used in EBSD were 20 kV and 200 nm, respectively.

Fig. 1(a) shows the EBSD image of the non-charged 304 specimen. There are more than twenty grains with various orientations in the chosen area. Fig. 1(b) and (c) show the CPD maps taken by SKPFM from the same area at $t = 2.5$ h and $t = 21$ h after the finishing of ion milling, respectively. Similar CPD distributions with small contrast between the grains with different crystallographic orientations are observed at different times. It is noted that the (111) and neighboring (111) grains are a little darker than the (001), (101) and their neighboring grains, indicating slightly higher work function of (111) grains than that of (001) and (101) grains, which is similar to the trend of decreasing in work function of the surface grains in fcc metals demonstrated by theoretical calculations [18,19]. The CPD profiles along the dark line aa′, which are superimposed to the CPD maps, indicate that the difference between the highest and lowest CPDs is within 0.005 V for a given scan. The average CPD along the line aa′ changes from -0.064 V at $t = 2.5$ h to -0.080 V at $t = 21$ h; the variation of 0.016 V is less than the fluctuation of the testing system with time (0.02 V). Therefore, for the specimen without HC, there is no significant change of CPD for these testing conditions.

Fig. 2(a) shows the EBSD image taken from the hydrogen-charged specimen. There are also about twenty grains with various orientations in the chosen area. Fig. 2(b)–(d) show the typical CPD maps taken at $t = 2.8$ h, $t = 44$ h, and after heating at 473 K, respectively. Fig. 2(e) shows the CPD curves taken along the dark line aa′ drawn in Fig. 2(a) at different times and after heating. The CPD curve taken from the non-charged specimen is also shown in Fig. 2(e) for reference. Fig. 2(f) shows the average CPDs of (111), (001) and (101) grains taken along the small white bars drawn in Fig. 2(a) as a function of time. The SKPFM measurement at $t = 2.8$ h reveals that the CPD distribution at the beginning of hydrogen release is similar to that of the non-charged specimen, showing lower CPDs of the (111) and neighboring (111) grains than that of the (001), (101) and their neighboring grains; however, the average CPD is 0.335 V, which is 0.399 V higher than that of the non-charged specimen at $t = 2.5$ h, and the difference of the CPD between (111), (001), and (101) grains is obviously larger than that in the non-charged specimen, as shown in Fig. 2(b), (e) and (f). With the increasing time, the average CPD is increased to a maximum of 0.373 V at $t = 4$ h, at which the difference of the CPD between (111), (001), and (101) grains becomes very small, as shown in Fig. 2(e) and
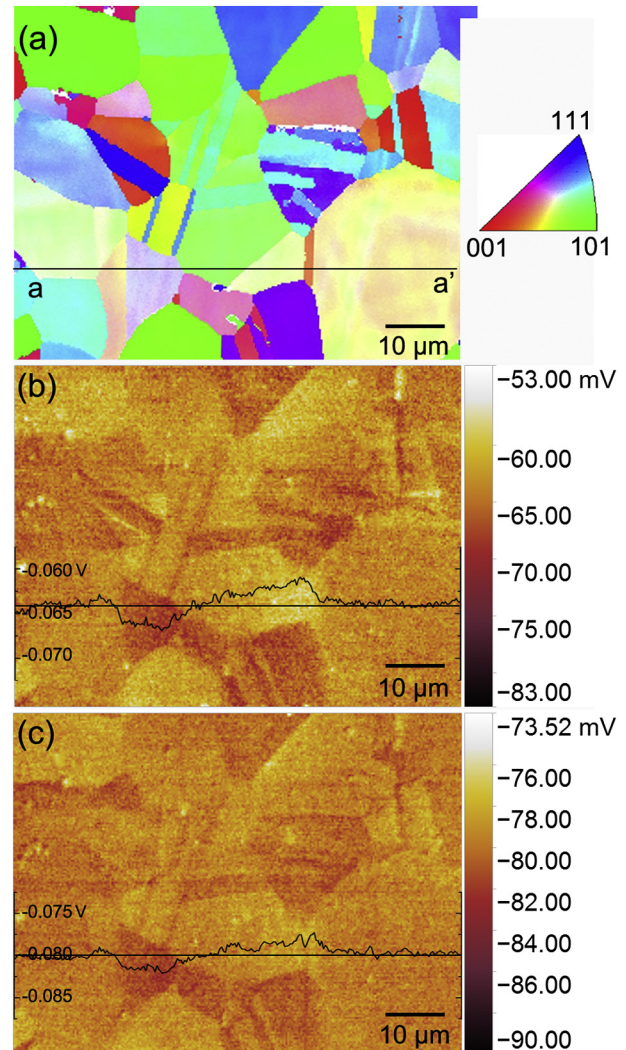

Fig. 1. EBSD and SKPFM results obtained from same area of non-charged specimen. (a) EBSD inverse pole image at Z direction which is normal to the surface. (b) and (c) CPD maps taken by SKPFM at $t = 2.5$ h and $t = 21$ h after ion milling treatment, respectively.

(f). With further increases of time, the average CPD is gradually decreased to 0.280 V at $t = 44$ h and the CPD distribution is reversed, showing higher CPD of the (111) and neighboring (111) grains than that of the (001), (101) grains and their neighbors, as shown in Fig. 2(c)–(f). The CPD drops of the (001) and (101) grains with time are significantly larger than that of the (111) grains but no obvious difference is observed between the (001) and (101) grains, as shown in Fig. 2(f). With further increases of time, only small changes are observed, indicating that many trapped and dissolved hydrogen atoms remain in the near surface area. After heating at 473 K for 2.5 h, the contrast of the CPD map is reversed again becoming similar to that of the non-charged specimen with an average CPD of -0.055 V, as shown in Fig. 2(d)–(f), and indicating that most of the hydrogen has escaped from the near surface area due to enhanced diffusion at the annealing temperature.

The behavior of hydrogen release from metals has been extensively studied and it is known that hydrogen concentration in the near surface area, including surface, is dynamically controlled by hydrogen desorption and segregation processes [20–22]. The hydrogen desorption rate can be described by $R_{des} = k\, C_s^n$, where R_{des} is desorption rate, k is rate coefficient for the desorption process, n is kinetic order of desorption and C_s is surface concentration [23]. The rate of hydrogen segregation in the near surface area, namely the SKPFM active volume, can be described by Fick's first law: $R_{seg} = D \frac{dC}{dx}$, where R_{seg} is segregation rate, D